the FEBS Journal

The effect of zinc oxide nanoparticles on the structure of the periplasmic domain of the *Vibrio cholerae* ToxR protein

Tanaya Chatterjee[1], Soumyananda Chakraborti[1], Prachi Joshi[2], Surinder P Singh[3], Vinay Gupta[4] and Pinak Chakrabarti[1]

1 Department of Biochemistry, Bose Institute, Kolkata, India
2 National Physical Laboratory, New Delhi, India
3 Department of Engineering Science and Materials, University of Puerto-Rico, Mayaguez, USA
4 Department of Physics and Astrophysics, University of Delhi, New Delhi, India

Keywords
nanoparticle–protein interaction; protein unfolding by nanoparticle; ToxR protein; *Vibrio cholerae*; zinc oxide nanoparticle

Correspondence
Department of Biochemistry, Bose Institute, P-1/12 CIT Scheme VIIM, Kolkata 700054, India
Fax: +91 33 2355 3886
Tel: +91 33 2569 3253
E-mail: pinak@boseinst.ernet.in

(Received 7 April 2010, revised 24 June 2010, accepted 3 August 2010)

doi:10.1111/j.1742-4658.2010.07807.x

Proteins adsorbed on nanoparticles (NPs) are being used as biosensors and in drug delivery. However, our understanding of the effect of NPs on the structure of proteins is still in a nascent state. In this work we report the unfolding behavior of the periplasmic domain of the ToxR protein (ToxRp) of *Vibrio cholerae* on zinc oxide (ZnO) nanoparticles with a diameter of 2.5 nm. This protein plays a crucial role in regulating the expression of several virulence factors in the pathogenesis of cholera. Thermodynamic analysis of the equilibrium of unfolding, induced both by urea and by guanidine hydrochloride (GdnHCl), and measured by fluorescence spectroscopy, revealed a two-state process. NPs increased the susceptibility of the protein to denaturation. The midpoints of transitions for the free and the NP-bound ToxRp in the presence of GdnHCl were 1.5 and 0.5 M respectively, whereas for urea denaturation, the values were 3.3 and 2.4 M, respectively. Far-UV CD spectra showed a significant change in the protein conformation upon binding to ZnO NPs, which was characterized by a substantial decrease in the α-helical content of the free protein. Isothermal titration calorimetry, used to quantify the thermodynamics of binding of ToxRp with ZnO NPs, showed an exothermic binding isotherm ($\Delta H = -9.8$ kcal·mol^{-1} and $\Delta S = -5.17$ cal·mol^{-1}·K^{-1}).

Introduction

Adsorption of proteins on solid surfaces, a topic of intense research activities in recent years, strongly depends on the nature of the protein, the surface geometry and the physicochemical characteristics of the solid surface [1–3]. Because of their small size, nanoparticles (NPs) can enter almost all areas of the body, including cells and organelles. In the biological milieu, they become coated with proteins, which may undergo conformational changes, thereby affecting the downstream regulation of protein–protein interactions, cellular signal transduction and transcription of DNA [4–7]. Conformational transition, leading to peptide aggregation and the formation of amyloid fibrils, has been implicated in the pathogenesis of several neurodegenerative diseases, and it has been shown that NPs with specific surface chemistry can inhibit the fibrillation of the disease-associated amyloid β protein (Aβ) [8,9]. Various specific and nonspecific interactions,

Abbreviations
GdnHCl, guanidine hydrochloride; ITC, isothermic titration calorimetry; NP, nanoparticle; pI, isoelectric point; ToxRp, periplasmic domain of ToxR; UV, ultraviolet; ZnO, zinc oxide.

such as electrostatic, hydrogen bonding and hydrophobic interactions, between the protein and the adsorbent determine how the structure and stability of proteins are affected [10–12]. Gold, silica and carbon nanotubes have been extensively used for protein attachment [13–16]. In this study, we chose zinc oxide (ZnO) NPs (which have received considerable attention because of their unique properties) as ultraviolet (UV) light-blocking materials, especially of light in the UV-A region [17,18]. It has recently been reported that ZnO NPs exhibit a strong preferential ability to kill cancerous T cells, compared with normal cells, by inducing apoptosis [19,20].

The causative agent of the endemic and epidemic disease cholera is the Gram-negative bacterium *Vibrio cholerae*, which contains a number of virulence genes, including cholera toxin (*ctxAB*), and several other genes involved in the pathogenesis of the organism, such as the accessory cholera enterotoxin (*ace*) and the zonula occludens toxin (*zot*). In *V. cholerae*, the signal-transduction protein ToxR functions as the regulator that controls the transcription of virulence genes, such as cholera toxin (*ctxAB*), by binding to the heptamer motif *TTATGAT* in the cholera toxin promoter [21,22]. It is an integral membrane protein (Swiss-Prot entry P15795), which is anchored in the membrane by a single membrane-spanning segment consisting of 16 amino acids, with its N- and C-terminal domains facing the cytoplasm (180 amino acid residues) and the periplasm (96 amino acid residues), respectively. To act as a transcriptional activator of *ctxAB*, ToxR requires the dimerization of its C-terminal periplasmic domain [23,24].

Usually, model enzymes, such as lysozyme, chymotrypsin, BSA, carbonic anhydrase and RNase A, or small electron-transfer proteins, such as cytochrome *c*, are used in studies with NPs [25–29]. Many more proteins of diverse functions need to be brought within the ambit of such studies to develop a coherent view of the applicability of NPs in biotechnology. Here we analyzed, using different spectroscopic methods, the conformational changes of the periplasmic domain of ToxR (ToxRp) [30] induced by the interaction with ZnO NPs of 2.5 nm in size (quite comparable to the size of the protein). Urea- and guanidine hydrochloride (GdnHCl)-induced unfolding curves of the free and the adsorbed ToxRp indicate a two-state process. The significant conformational changes induced by ZnO NPs may be attributed to strong electrostatic interactions between the protein and the NPs. This work, we believe, is the first attempt to quantify the impact of ZnO NPs upon the stability of any transcriptional activator.

Results and Discussion

For an improved engineering of NPs with favorable bioavailability and biodistribution, it is essential to have an in-depth knowledge of the mechanism(s) of association and interaction of proteins with the particle surface and the consequent effect on the structure of the protein. Towards achieving this goal we studied the effect of ZnO NPs on the structure of ToxRp, alone and in the presence of denaturing agents, and determined the thermodynamic parameters of binding. ToxRp is the 96-residue C-terminal domain of the intact ToxR protein, which has a cytoplasmic region at the N-terminus and a short membrane-spanning region in the middle. ToxRp is a dimeric protein and the oligomeric state is stabilized by an intersubunit disulfide bond involving Cys293 [30]. The elution profile of analytical gel filtration of the NP-treated protein was very similar to that of the free protein, which confirms that the dimeric nature of the protein remains unperturbed in the presence of NPs (Fig. S1), as can indeed be expected as a result of the presence of a disulfide bridge linking the two subunits. Assuming a 1 : 1 stoichiometry of ToxRp and NP, the surface concentration of the protein on NPs was found to be 70 $\mu g \cdot cm^{-2}$ (see the Materials and methods for details).

Intrinsic tryptophan fluorescence

Tryptophan fluorescence is a sensitive monitor providing information on the structural and dynamic properties of protein. Protein fluorescence spectra with a maximum of around 335 nm are characteristic of tryptophan residues buried well within the hydrophobic core, whereas a spectral maximum of around 350–355 nm indicates tryptophan residues exposed to the solvent [31,32]. ToxRp contains only one tryptophan residue (at position 31), which simplifies the interpretation of fluorescence changes in the protein. The fluorescence-emission spectra of ToxRp were measured in both the presence and the absence of ZnO NPs. The tryptophan fluorescence was also investigated in the presence of chaotropic agents such as urea and GdnHCl.

The fluorescence-emission spectrum of free ToxRp showed a wavelength maximum at 342 nm. On conjugation to ZnO NPs (size 2.5 nm), the fluorescence intensities of the free ToxRp, as well as of the urea- and GdnHCl-treated ToxRp, were reduced considerably (Fig. 1). For the free ToxRp, upon increasing the concentration of urea or GdnHCl, the wavelength maxima shifted to higher wavelengths (the transition curves are shown in Figs 2 and 3). At about 5 M urea

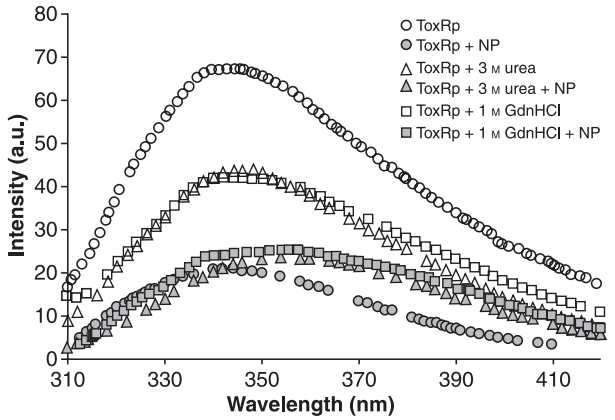

Fig. 1. Fluorescence emission spectra (λ_{ex} = 295 nm) of free and ZnO NP-treated ToxRp in the presence and absence of GdnHCl and urea.

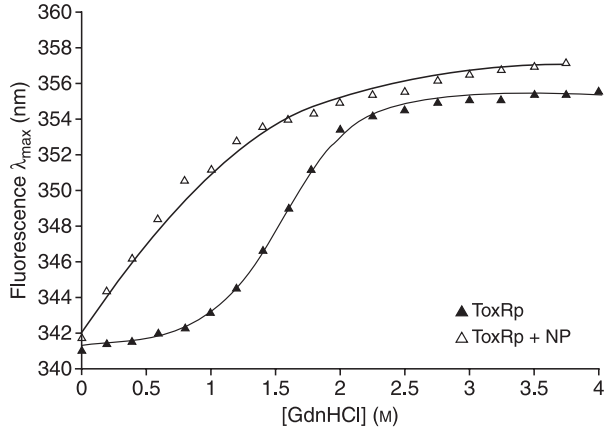

Fig. 2. Shift in wavelength (λ_{max}) of free and NP-conjugated ToxRp at pH 8.0 and 25 °C with increasing concentration of GdnHCl.

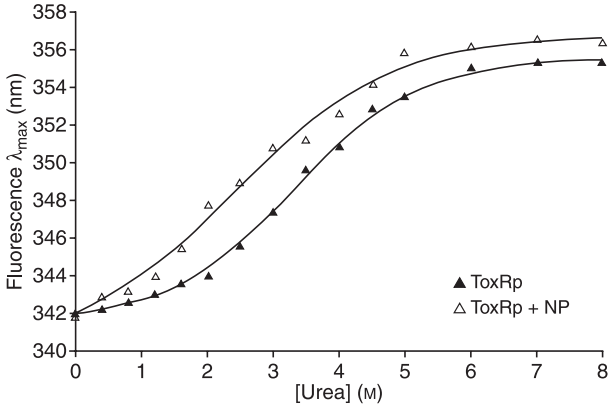

Fig. 3. Shift in wavelength (λ_{max}) of free and NP-adsorbed ToxRp at pH 8.0 and 25 °C with increasing concentration of urea.

and 2.5 M GdnHCl, the spectrum exhibited a peak at around 356 nm. The decrease in fluorescence intensity accompanied by the red shift indicates exposure of the Trp residue to the aqueous environment [31].

Compared with free ToxRp, the ToxRp–NP conjugates were more vulnerable to increasing concentrations of either of the chaotropic agents, as reflected in the significant loss of fluorescence intensity and the increase in λ_{max}. Whereas the free ToxRp exhibited a λ_{max} of 343 nm in the presence of 1 M GdnHCl, the value was 352 nm for the NP-treated protein at the same concentration of GdnHCl. The urea-induced transition curve for ToxRp bound to ZnO NPs showed complete denaturation (λ_{max} = 350 nm) when the ToxRp–NP conjugates were exposed to 3 M urea, a concentration at which the free ToxRp showed a λ_{max} of 347 nm. The unfolding free-energy (ΔG_{NU}) values were lower for NP-treated ToxRp than for free ToxRp, in the presence of either urea or GdnHCl, as shown in Table 1. Dividing ΔG_{NU} by the slope gives the value for the midpoint of unfolding transition. The $[GdnHCl]_{1/2}$ (denaturant concentration corresponding to the mid-point of transition) for free ToxRp was 1.5 M, whereas that for the NP-conjugated ToxRp was 0.5 M. By contrast, the $[urea]_{1/2}$ for free ToxRp was 3.3 M, as opposed to 2.4 M for the NP-bound ToxRp. Hence, ToxRp becomes more denatured upon binding to ZnO NPs and the effect is more severe in the presence of GdnHCl.

Quenching of tryptophan fluorescence by acrylamide, a collisional quencher, has been widely used to study the tryptophan environment in proteins [33]. To assess the solvent accessibility of the single tryptophan residue of ToxRp, fluorescence experiments were carried out using acrylamide, which quenches on the basis of physical collision with the excited indole ring of tryptophan. Figure 4 shows the Stern–Volmer plot for the quenching of tryptophan fluorescence of free ToxRp and ToxRp–ZnO NP conjugates, as well as of the samples in the presence of the chaotropic agents GdnHCl and urea. The Stern–Volmer constants, K_{SV}, calculated from the plots, were 5.5 and 7.9 M^{-1} for the free and the NP-conjugated ToxRp, respectively. In the presence of either of the chaotropic agents, *viz*. 1 M GdnHCl or 3 M urea, a significant increase in the quenching efficiency was observed compared with free ToxRp, as indicated by the increase in K_{SV} to 6.6 and 7.5 M^{-1}, respectively. A further increase in the quenching efficiency was noted for the NP-bound ToxRp in the presence of 1 M GdnHCl (K_{SV} 21.7 M^{-1}) as well as in the presence of 3 M urea (K_{SV} 23.9 M^{-1}). A moderate K_{SV} value for free ToxRp confirmed the presence of a buried tryptophan residue, whose accessibility

Table 1. Two-state analysis of the unfolding of ToxRp using GdnHCl or urea, performed in the presence and the absence of ZnO NP.

	GdnHCl		Urea	
	ToxRp	ToxRp + ZnO NP	ToxRp	ToxRp + ZnO NP
ΔG_{NU} (kcal·mol^{-1})	3.14 ± 0.14	0.98 ± 0.02	2.05 ± 0.07	1.18 ± 0.09
m_{NU} (kcal·mol^{-1}·M^{-1})	2.03 ± 0.08	1.96 ± 0.09	0.62 ± 0.12	0.49 ± 0.12
$[d_{NU}]_{1/2}$ (M)[a]	1.54	0.49	3.30	2.40

[a] Denaturant concentration corresponding to the midpoint of the transition.

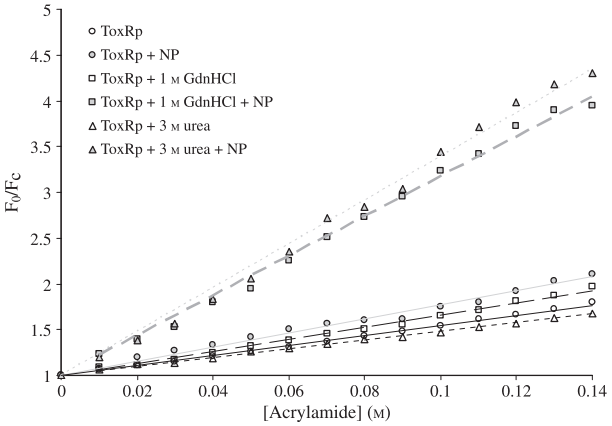

Fig. 4. Acrylamide quenching of tryptophan fluorescence of free and NP-treated ToxRp in the presence and absence of chaotropic agents such as 1 M GdnHCl and 3 M urea.

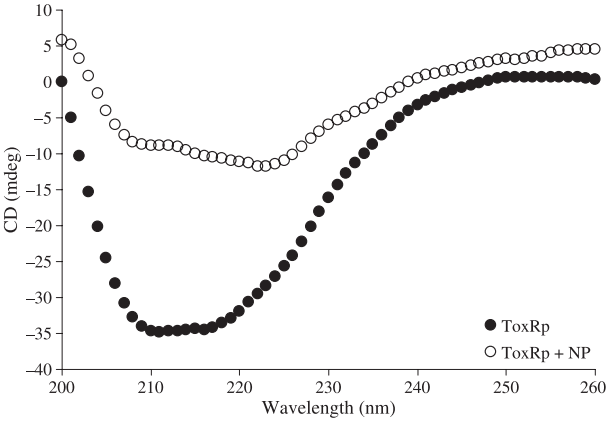

Fig. 5. Far-UV CD spectra of ToxRp (10 μM in 0.1 M potassium phosphate buffer, pH 8.0) in the absence and presence of ZnO NPs.

increased upon adsorption onto ZnO NPs, as evident from the higher K_{SV} value. The values of K_{SV} are about three times larger for adsorbed ToxRp in the presence of either of the chaotropic agents, indicating a higher accessibility of the quencher to the tryptophan as it becomes exposed by the unfolding of the protein.

CD measurements

Far-UV CD spectroscopy is one of the most commonly used techniques used to analyze secondary structure and to monitor the structural changes occurring in proteins in response to external factors [34,35]. Figure 5 depicts the far-UV CD spectra of free ToxRp as well as of ToxRp–ZnO conjugates. A large negative ellipticity for free ToxRp, of between 210 and 230 nm, is indicative of the presence of α-helix, and the secondary structural content was estimated by deconvolution of the CD data using CDNN, which employs a neural network algorithm [36,37]. The results showed that free ToxRp has an α-helical content of 27% and a random coil content of 39%. These estimates can be compared with the predicted values of 26% α-helix and 41% of coil (Fig. S2), obtained by applying the secondary structure prediction program PSIPRED to the amino acid sequence of the protein [38]. On becoming bound to ZnO NPs (Fig. 5), a significant percentage of secondary structure was lost – the α-helical content decreased to 18% with a concomitant increase in random coil to 47%. Hence, ToxRp undergoes a significant reduction in secondary structure content upon adsorption onto ZnO NPs.

It has been previously reported that GdnHCl is a much stronger denaturing agent than urea; upon consideration of the midpoint of transition for protein unfolding, the relationship $[urea]_{1/2} = 2[GdnHCl]_{1/2}$ is generally valid for globular proteins [39,40]. When studying the unfolding of ribonuclease A, GdnHCl was found to be 2.8 times more effective than urea, whereas for lysozyme it was 1.7 times more effective than urea [41]. Although the $GdnH^+$ ion and urea are very similar structurally (as both have a planar structure), the former has a positive charge that is delocalized over the planar structure. So, the key factor may be the difference in ionic character, which leads to preferential binding of the $GdnH^+$ ion on the surface of the protein that subsequently weakens and perturbs the electrostatic interactions stabilizing the native structure [42]. For ToxRp, the $[urea]_{1/2}$ value is about twice that of the $[GdnHCl]_{1/2}$ value, but for the

NP-bound ToxRp it is almost five times higher (Table 1), showing that together with NP, GdnHCl is a more potent denaturing agent than urea. For the NP-treated ToxRp, GdnHCl behaves as a classical denaturant, even at a concentration as low as 1 M (Fig. 2).

Thermal unfolding of the free and the ZnO NP-conjugated ToxRp was monitored by far-UV CD spectroscopy. The unfolding process induced by increasing the temperature was studied following the ellipticity at 222 nm, as shown in Fig. 6. The results are reported in terms of the mean residue ellipticity ($[\theta]$, deg·cm^2·dmol^{-1}), which is given by:

$$[\theta_{222}] = \frac{100\theta Mw}{clN}, \quad (1)$$

where $[\theta_{222}]$ is the measured ellipticity in degrees, c is the protein concentration in mg/mL, l is the path length in cm, M_W is the molecular weight of ToxRp and N is the number of amino acid residues of ToxRp. Considering that ToxRp undergoes a two-state transition between folded (F) and unfolded (U) forms, the equilibrium constant (K) at any temperature (T) can be written as:

$$K = \frac{[F]}{[U]}, \quad (2)$$

where $[F]$ and $[U]$ are the concentrations of the folded and unfolded forms, respectively. The equilibrium constant, K, is related to the Gibbs free energy of unfolding as:

$$\Delta G = -RT \ln K, \quad (3)$$

where R is the gas constant and T is the absolute temperature.

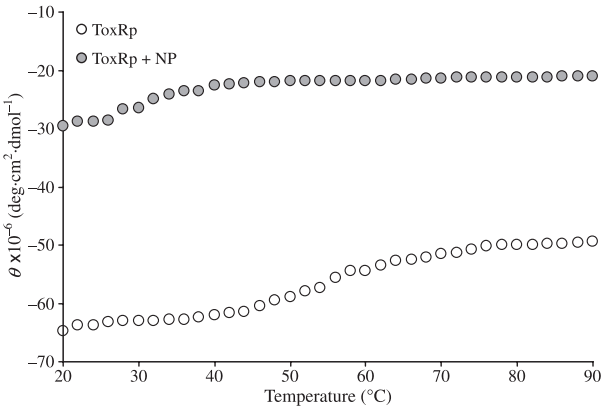

Fig. 6. Variation of ellipticity at 222 nm with temperature.

Again, the fraction folded at any temperature α is given by:

$$\alpha = \frac{[F]}{[F] + [U]}, \quad (4)$$

which is $K/(1 + K)$ and:

$$\alpha = \frac{\theta_T - \theta_U}{\theta_F - \theta_U}, \quad (5)$$

where θ_T is the observed ellipticity at any temperature T, θ_F is the ellipticity of the fully folded form and θ_U is the ellipticity of the unfolded form. To fit the change of CD at a single wavelength as a function of temperature T, the Gibbs–Helmholtz equation was used:

$$\Delta G = \Delta H(1 - T/T_M) - \Delta C_p T_M [1 - (T/T_M) + (T/T_M)\ln(T/T_M)], \quad (6)$$

where T_M is the melting temperature, ΔH is the change in enthalpy and ΔC_p is the change in specific heat capacity from the folded to the unfolded state. Temperature-dependent far-UV CD studies showed discrete changes of adsorbed ToxRp compared with free protein, which was characterized by a decrease in molar ellipticity. By curve fitting, the transition temperatures were found to be 54 °C for free ToxRp and 33 °C for NP-conjugated ToxRp, respectively.

Effect of ionic strength on binding of ToxRp to ZnO NP

If the interaction between a protein and an NP involves complementary electrostatic surface recognition, the ionic strength of the medium would be expected to have an effect on the binding [43]. To study the effect of ionic strength on the conformation of ToxRp in the presence of ZnO NP, CD experiments were carried out in the presence of 0.1, 0.5 and 1 M KCl. The helical content of the free protein, as indicated by the θ_{222} value, increased with the addition of KCl and reached a maximum at 0.5 M KCl, beyond which further addition of KCl did not seem to have any effect (Fig. 7). NPs have a strong destabilization effect on the structure of ToxRp. However, in the presence of KCl the structure was retained, and in fact, an increase in the helical content was found (similar to that observed for the free protein). Likewise, the effect of pH on the ToxRp–NP interaction was also studied. However, both CD and fluorescence data

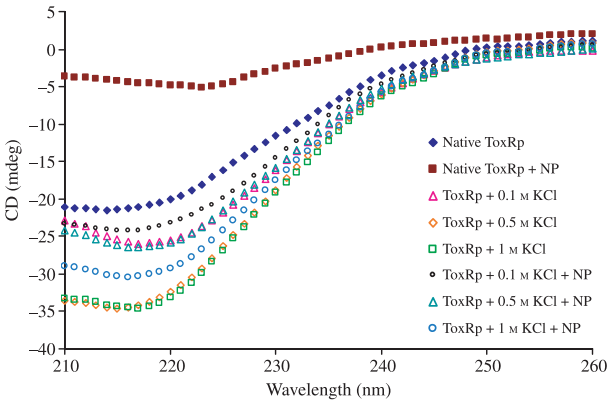

Fig. 7. Far-UV CD spectra of ToxRp in the presence of varying concentrations of KCl in the absence and presence of ZnO NPs.

(Fig. S3) indicated that the effect of NPs on the protein structure was not influenced by pH.

Results from isothermal titration calorimetry and the nature of interaction

Isothermal titration calorimetry (ITC) has been used to assess the affinity and stoichiometry of protein binding to NPs, directly providing the free energy and enthalpy of association, whose values then lead to the change in entropy for the process [44–46]. The thermodynamic parameters for the interaction between ToxRp and ZnO NPs (Fig. 8) are summarized in Table 2. The interaction involves about two NPs to one ToxRp and has a favorable enthalpy change ($\Delta H < 0$) that is offset partially by an unfavorable entropy ($\Delta S < 0$), affording a total free-energy change of −8.3 kcal·mol^{-1}. The stoichiometry may be explained by the dimeric structure of the protein providing two binding sites to NP. A negative ΔH signifies more favorable noncovalent (such as electrostatic, hydrogen bonding, van der Waals etc.) interactions between the protein and NPs than between the two components taken separately and water. The unfavorable negative-entropy change may arise from the conformational restriction of the flexible amino acids of ToxRp, but it also indicates a lesser contribution of hydrophobic interactions (which causes an increase in solvent entropy as a result of the release of water upon binding and burial of hydrophobic groups). The free-energy change associated with the binding is quite similar to that seen in the lysozyme–ZnO NP interaction [22] and those between other proteins and amino acid functionalized gold NPs [47].

The ToxRp protein has an isoelectric point (pI) of 5.84 (the theoretical value calculated using the ProtParam program) [48]. By contrast, the pI of ZnO is ~ 9.5 [49,50]. Consequently, under the experimental condition (pH 8.0) the acidic groups on the protein would be negatively charged, whereas ZnO NP would become

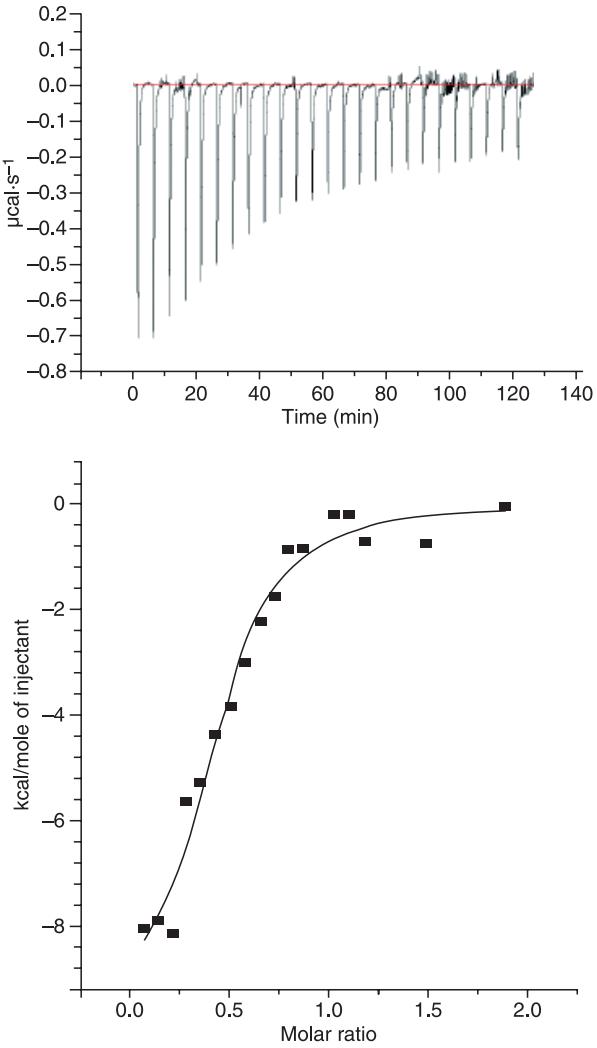

Fig. 8. ITC data from the titration of 160 µM ToxRp in the presence of 16 µM ZnO NP. Heat flow versus time during the injection of ToxRp at 30 °C (upper panel) and the heat evolved per mol of added ToxRp (corrected for the heat of dilution of the protein) against the molar ratio (ToxRp to NP) for each injection (lower panel). The data were fitted to a standard model.

Table 2. Thermodynamic parameters for the binding of ToxRp to ZnO NPs, derived from ITC measurements.

Parameter	Value (± SD)
n (NP: protein stoichiometry)	2.27 ± 0.02
K (binding constant, M^{-1})	(0.9 ± 0.3) × 10^6
$\triangle H$ (binding enthalpy, kcal per mol)	−9.8 ± 0.8
$\triangle S$ (entropy change, cal per mol·K)	−5.17
$\triangle G$ (free energy change, kcal per mol)	−8.3

positively charged by the absorption of H^+ from the medium, and the ensuing electrostatic interaction would lead to a degradation of the native structure. Because of the lack of homology with any known structure, the three-dimensional structure of ToxRp could not be ascertained. However, the secondary-structure predictions (Fig. S2) indicate the presence of a large number of charged residues in the coil/loop regions of the molecule, which are likely to be perturbed by NPs. The predominant contribution of electrostatic interactions, along with van der Waals interactions, rather than hydrophobic interactions, is manifested as the higher contribution of enthalpy, compared with entropy, in the free energy of binding. That the electrostatic interaction is important is also revealed by the effect of salt on the ToxRp–NP interaction, with the protein retaining more of its secondary structures in the presence of salt than in its absence (Fig. 7), indicating the inhibitory role of salt on the interaction. The periplasmic domain of ToxR has been shown to be less compact than the cytoplasmic domain of the same protein [30], and is possibly prone to disturbance by charged NPs.

Proteins may be classified as 'hard' or 'soft' depending on the resistance of the protein to conformational changes in the presence of NPs [51–53]. The proteins that readily undergo conformational changes after adsorption onto NPs are designated as 'soft' and those that can resist conformational changes are 'hard'. ToxRp should be classified as 'soft' in its behavior towards ZnO NP. The acidic pI and a relatively less compact structure [30] of the protein, along with the distribution of the charged groups on various loops/nonregular regions of the molecule, seem to be ideal for triggering conformational changes upon adsorption to positively charged NPs. For such proteins, NPs elicit the same behavior as that of a chaotropic agent. By contrast, a ZnO NP, of size 7 nm, increased the helical content of lysozyme and stabilized the structure against denaturation by chaotropic agents [25]**.** This was caused by the proposed binding of the NP at the active-site cleft such that the spherical surface of NP was complementary to the concave surface of the protein, and tight binding could be achieved without any large-scale conformational adjustment.

Conclusions

In this work we showed that binding to ZnO NPs can result in major structural changes of the ToxRp protein of *V. cholerae*. Based on the thermodynamic parameters of binding one can speculate on the nature of the interaction between ToxRp and ZnO NPs, and the consequent effect on protein conformation. The NP-treated protein is more susceptible to denaturation by chaotropic agents. Relating the affinity of proteins to NPs would pave the way for NPs being used as biosensors and in drug delivery.

Materials and methods

Materials

Acrylamide, urea, GdnHCl and glycerol were purchased from Sigma Chemicals (St Louis, MO, USA). All other chemicals, obtained from Merck (Mumbai, India), were of analytical grade.

ZnO NPs

The colloidal ZnO NPs used in this study were synthesized by the modified sol-gel route using zinc acetate dihydrate [$Zn(CH_3COO)_2{\cdot}2H_2O$], and sodium hydroxide was used as a precursor [54]. Zinc acetate (10 mM) was refluxed in ethanol for 20 min to obtain a clear solution that was allowed to cool to room temperature. Then, 20 mM NaOH was sonicated in ethanol and added dropwise to the zinc acetate solution with continuous stirring. The ZnO NPs were precipitated using *n*-hexane and centrifuged. Spherical ZnO NPs, of diameter 2.5 nm [54], were obtained by washing the precipitate with ethanol and then drying at 60 °C. The particles are stable in solutions at pH 8.

Isolation and purification of ToxRp

Cloning, expression and purification of the ToxRp protein was carried out as previously reported [30]. The purity of ToxRp was verified by SDS/PAGE, followed by staining with Coomassie Blue, which identified a single band indicating that the protein was essentially pure. The protein concentration was measured spectrophotometrically at 280 nm using a molar extinction coefficient (ε) of 8604 $M^{-1}{\cdot}cm^{-1}$.

Preparation of samples

All samples were prepared in 0.1 M potassium phosphate buffer (pH 8.0). A 10 μM concentration of ToxRp was used in all experiments. Before use, the protein solution was exhaustively dialyzed in 0.1 M potassium phosphate buffer (pH 8.0) using membrane tubing (Spectra biotech membrane MWCO: 3500; Spectrum Lab, Rancho Dominguez, CA, USA) at 4 °C. As ZnO NPs have a tendency to form aggregates in solution, as revealed by a dynamic light-scattering experiment (data not shown), the colloidal suspension of ZnO was sonicated extensively before use. A 1 : 1 molar ratio of NPs and ToxRp was used to study the NP–ToxRp interaction, and the samples were incubated at

37 °C overnight. Stock samples of the chemical denaturants urea and GdnHCl (both 10 M) were prepared immediately before use. Different amounts of these solutions were mixed with ToxRp and the mixture was then incubated overnight at 25 °C. The final concentrations ranged from 0 to 8 M for urea and from 0 to 6 M for GdnHCl. Each sample was mixed thoroughly with a different concentration of the denaturating agent in the presence and absence of ZnO NPs.

Analytical gel-filtration chromatography

Gel-filtration chromatography was performed to investigate the oligomeric status of ToxRp after interacting with ZnO NPs. Analytical gel-filtration experiments were carried out in an HPLC system (Waters) using a Bio-Sil SEC 250-5 column (7.8 mm × 300 mm, Bio-Rad, CA). Protein samples, at a concentration of 1 $\mu g \cdot \mu L^{-1}$, were injected one at a time. The column was pre-equilibrated with 0.1 M potassium phosphate buffer (pH 7.2) at a flow rate of 0.5 mL/min. The protein/ZnO NP ratio was maintained at 1 : 1 and incubated at 37 °C overnight before loading onto the column.

Fluorescence measurements

Fluorescence spectra were recorded using a Hitachi F–3010 spectrofluorimeter fitted with a spectra addition and subtraction facility. Slit widths with a band-pass of 5 nm were used for both excitation and emission. Samples were placed in a 1-cm path-length quartz cuvette in the spectrophotometer, and intrinsic fluorescence-emission spectra of ToxRp were recorded from 310 to 410 nm as a function of varying concentrations of chaotropic agents and/or NP. An excitation wavelength of 295 nm was used to follow tryptophan fluorescence. The wavelengths at maximum emission intensity (λ_{max}) and the fluorescence intensity at 340 nm were determined. For the denaturation study, a series of freshly prepared solutions of different concentrations of GdnHCl and urea in 0.1 M potassium phosphate buffer (pH 8.0) were prepared and ToxRp was added to a final concentration of 10 μM. Blank controls were produced by adding the same volume of buffer, but with no protein, to the same volume of GdnHCl and urea solutions.

Quenching of tryptophan fluorescence with acrylamide was conducted by the addition of small aliquots of 1 M stock solution to the cuvette; measurements were taken 30 s later and dilution was taken into account. The Stern–Volmer equation used for acrylamide quenching of tryptophan fluorescence is:

$$\frac{F_0}{F_C} = 1 + K_{SV}[Q], \tag{7}$$

where F_0 is the initial fluorescence intensity, F_C is the corrected intensity in the presence of quencher and K_{SV} is the Stern–Volmer constant.

Analysis of unfolding data

Unfolding of free and NP-treated ToxRp was monitored by fluorescence λ_{max} (λ_{ex} = 295 nm), as a function of the concentration of urea and of GdnHCl. Analysis of denaturant-induced unfolding curves followed a simple two-state transition between the folded and unfolded states, N and U respectively. At each denaturant concentration the observed signals, S, representing the shift of the fluorescence emission maxima, were fitted to a two-state equation, as shown below:

$$S = \frac{S_N e^{\left(\frac{\Delta G_{NU}}{RT}\right)} + S_U}{e^{\left(\frac{\Delta G_{NU}}{RT}\right)} + 1} \tag{8}$$

The unfolding free-energy (ΔG_{NU}) was assumed to vary linearly with the concentration of denaturant, [d_{NU}], as:

$$\Delta G_{NU} = \Delta G_{NU}^{H_2O} - m_{NU}[d_{NU}]_{1/2} \tag{9}$$

The constant m_{NU} is related to the difference in solvent-accessible surface area between the unfolded and the folded states of the protein.

CD spectroscopy

The far-UV CD spectra (200–260 nm) of free ToxRp and and NP-treated ToxRp were recorded on a JASCO J600 spectropolarimeter, equipped with a Peltier-type temperature controller and a thermostated cell holder, using a quartz cuvette of 1 mm path-length. Scans were taken from 200 to 260 nm at a rate of 5 $nm \cdot min^{-1}$, with a 0.1-step resolution and 4-s responses. In all measurements, a protein concentration of 10 μM was used in 0.1 M potassium phosphate buffer (pH 8.0). CD spectra of the ZnO NPs in phosphate buffer were recorded exactly as for the text samples, as a control. The weak CD signal of ZnO NPs was subtracted from that of the complex. At least three CD spectra were acquired for each sample and the spectra were averaged. Thermal-denaturation experiments were carried out by increasing the temperature from 20 to 90 °C, allowing temperature equilibration for 5 min before recording each spectrum.

ITC

The ITC experiment was carried out on a VP-ITC microcalorimeter (Microcal, Northampton, MA) at 30 °C. The protein was thoroughly dialysed for 24 h in 0.1 M potassium phosphate buffer (pH 8.0) before loading. Titration experiments consisted of 25 successive injections of ToxRp protein (injection volume 10 μL; concentration 160 μM) into the reaction cell (1.4 mL) containing ZnO NPs (concentration 16 μM) in 0.1 M potassium phosphate buffer (pH 8.0). The titration cell was stirred continuously at 310 rpm. The heat of dilution of the protein solutions when added to the

buffer solution in the absence of NPs was determined using the same number of injections and concentration of protein as in the titration experiments. The data were analyzed using a simple one-site binding model using MICROCAL ORIGIN 7.0 software (OriginLab Corporation, Northampton, MA) provided with the instrument. The binding constants (K), enthalpy changes (ΔH) and binding stoichiometries (n) were determined from curve-fitting analyses.

Measurement of surface concentration of ToxRp on ZnO NP

In this experiment, the amount of ToxRp on the ZnO NP surface was measured by UV spectroscopy. ToxRp protein (10 μM) was incubated at 37 °C for 6 h with different molar ratios of ZnO NPs (1 : 0.25, 1 : 0.5, 1 : 0.75 and 1 : 1) in 0.1 M potassium phosphate buffer (pH 8.0). The suspension was then centrifuged at 5000 ***g*** and the concentration of the protein in the supernatant was measured spectrophotometrically at 280 nm using a Shimadzu UV-2401 spectrophotometer (Shimadzu Corporation, Kyoto, Japan). The difference between the initial and final concentrations of ToxRp gave the amount of adsorbed protein on the surface of the ZnO NP [28]. For derivation of the surface area of NPs, the following equation was used:

$$a = \frac{3w\phi}{\rho R}, \qquad (10)$$

where a is the total area of the ZnO NP, w is the mass of ZnO, ϕ is the mass fraction of the NP (0.015), R is the radius (1.25 nm) and ρ is the density (0.015 g·cm^{-3}).

Acknowledgements

T.C. and P.C. are supported by grants from the Department of Science and Technology. S.P. acknowledges the funding from IFN-EPSCoR. We thank Prof. B. Bhattacharyya for the use of the ITC facility.

References

1 Hobora D, Imabayashi SI & Kakiuchi T (2002) Preferential adsorption of horse heart cytochrome c on nanometer-scale domains of a phase-separated binary self-assembles monolayer of 3-mercaptopropionic acid and 1-hexadecanethiol on Au (III). *Nano Lett* **2**, 1021–1025.

2 Roach P, Farrar D & Perry CC (2005) Surface tailoring for controlled protein adsorption: effect of topography at the nanometer scale and chemistry. *J Am Chem Soc* **127**, 8168–8173.

3 Vertegal AA, Siegel RW & Dordick JS (2004) Silica nanoparticle size influences the structure and enzyme activity of adsorbed lysozyme. *Langmuir* **20**, 6800–6807.

4 Nel AE, Madler L, Velegol D, Xia T, Hoek EMV, Somasundaran P, Klaessig F, Castranova V & Thompson M (2009) Understanding biophysicochemical interactions at the nano-bio interface. *Nat Mater* **8**, 543–557.

5 Thomas M & Klibanov AM (2003) Conjugation to gold nanoparticles enhances polyethyleneimine's transfer of plasmid DNA into mammalian cells. *Proc Natl Acad Sci USA* **100**, 9138–9143.

6 Zinchenko A, Luckel F & Yoshikawa K (2007) Transcription of giant DNA complexed with cationic nanoparticles as a simple model of chromatin. *Biophys J* **92**, 1318–1325.

7 Hellstrand E, Lynch I, Andersson A, Drakenberg T, Dahlbäck B, Dawson KA, Linse S & Cedervall T (2009) Complete high-density lipoproteins in nanoparticle corona. *FEBS J* **276**, 3372–3381.

8 Cabaleiro-Lago C, Quinlan-Pluck F, Lynch I, Lindman S, Minogue AM, Thulin E, Walsh DM, Dawson KA & Linse S (2008) Inhibition of amyloid beta protein fibrillation by polymeric nanoparticles. *J Am Chem Soc* **130**, 15437–15443.

9 Rocha S, Thünemann AF, do Carmo Perira M, Coelho M, Möhwald H & Brezesinski G (2008) Influence of fluorinated and hydrogenated nanoparticles on the structure and fibrillogenesis of amyloid beta-peptide. *Biophys Chem* **137**, 35–42.

10 Lynch I & Dawson KA (2008) Protein-nanoparticle interactions. *Nanotoday* **3**, 40–47.

11 Billsten P, Freskgard PO, Carlsson U, Jonsson BH, Olofsson G & Elwing H (1997) Adsorption to silica nanoparticles of human carbonic anhydrase II and truncated forms induce a molten-globule-like structure. *FEBS Lett* **402**, 67–72.

12 Aggarwal P, Hall JB, McLeland CB, Dobrovolskaia MA & McNeil SE (2009) Nanoparticle interaction with plasma proteins as it relates to particle biodistribution, biocompatibility and therapeutic efficacy. *Adv Drug Delivery Rev* **61**, 428–437.

13 Daniel MC & Astruc D (2004) Gold nanoparticles: assembly, supramolecular chemistry, quantum-size-related properties, and applications toward biology, catalysis and nanotechnology. *Chem Rev* **104**, 293–346.

14 Han G, Ghosh P, De M & Rotello VM (2007) Drug and gene delivery using gold nanoparticles. *Nanobiotechnology* **3**, 40–45.

15 Lundqvist M, Sethson I & Jonsson BH (2004) Protein adsorption onto silica nanoparticles: conformational changes depend on the particles' curvature and protein stability. *Langmuir* **20**, 10639–10647.

16 Asuri P, Bale SS, Pangule RC, Shah DA, Kane RS & Dordick JS (2007) Structure, function, and stability of enzymes covalently attached to single-walled carbon nanotubes. *Langmuir* **23**, 12318–12321.

17 Singh SP, Arya SK, Pandey P, Malhotra BD, Saha S, Sreenivas K & Gupta V (2007) Cholesterol biosensors

based on rf sputtered zinc oxide nanoporous thin film. *Appl Phys Lett* **91**, 063901.
18 Wu YL, Lim CS, Fu S, Tok AIY, Lau HM, Boey FYC & Zeng XT (2007) Surface modifications of ZnO quantum dots for bio-imaging. *Nanotechnology* **18**, 215604.
19 Hanley C, Layne J, Punnoose A, Reddy KM, Coombs I, Coombs A, Feris K & Wingett D (2008) Preferential killing of cancer cells and activated human T cells using ZnO nanoparticles. *Nanotechnology* **19**, 1–10.
20 Nie S, Xing Y, Kim GJ & Simons JW (2007) Nanotechnology applications in cancer. *Annu Rev Biomed Eng* **9**, 257–288.
21 DiRita VJ (1992) Co-ordinate expression of virulence genes of ToxR in *Vibrio cholerae*. *Mol Microbiol* **6**, 451–458.
22 Miller VL & Mekalanos JJ (1984) Synthesis of cholera toxin is positively regulated at the transcriptional level by *toxR*. *Proc Natl Acad Sci USA* **81**, 3471–3475.
23 Miller VL, Taylor RK & Mekalanos JJ (1987) Cholera toxin transcriptional activator ToxR is a transmembrane DNA binding protein. *Cell* **48**, 271–279.
24 Ottermann KM, DiRita VJ & Mekalanos J J (1992) ToxR proteins with substitutions in residues conserved with OmpR fail to activate transcription from the cholera toxin promoter. *J Bacteriol* **174**, 6807–6814.
25 Chakraborti S, Chatterjee T, Joshi P, Poddar A, Bhattacharyya B, Singh SP, Gupta V & Chakrabarti P (2010) Structure and activity of lysozyme on binding to ZnO nanoparticles. *Langmuir* **26**, 3506–3513.
26 Sousa SR, Moradas-Ferreira P, Saramago B, Melo LV & Barbosa MA (2004) Human serum albumin adsorption on TiO_2 from single protein solutions and from plasma. *Langmuir* **20**, 9745–9754.
27 Shang W, Nuffer JH, Dordick JS & Siegel RW (2007) Unfolding of Ribonuclease A on silica nanoparticle surfaces. *Nano Lett* **7**, 1991–1995.
28 Wu X & Narsimhan G (2008) Effect of surface concentration on secondary and tertiary conformational changes of lysozyme adsorbed on silica nanoparticles. *Biochim Biophys Acta* **1784**, 1694–1701.
29 Karlsson M, Martensson LG, Jonsson BH & Carlsson U (2000) Adsorption of human carbonic anhydrase II variants to silica nanoparticles occur stepwise: binding is followed by successive conformational changes to a molten-globule-like state. *Langmui* **16**, 8470–8479.
30 Chatterjee T, Saha R & Chakrabarti P (2007) Structural studies on *Vibrio cholerae* ToxR periplasmic and cytoplasmic domains. *Biochim Biophys Acta* **1774**, 1331–1338.
31 Lakowicz JR (1999) *Principles of Fluorescence Spectroscopy*. Plenum Publishing Corporation, New York.
32 Dockal M, Carter DC & Ruker F (2000) Conformational transitions of the three recombinant domains of human serum albumin depending on pH. *J Biol Chem* **275**, 3042–3050.
33 Eftink MR & Ghiron CA (1976) Fluorescence quenching studies with proteins. *Biochemistry* **15**, 672–680.
34 Greenfield NJ (2006) Using circular dichroism collected as a function of temperature to determine the thermodynamics of protein unfolding and binding interactions. *Nat Protoc* **1**, 2527–2535.
35 Venyaminov SY, Yu S & Yang JT (1996) *Circular Dichroism and the Conformational Analysis of Biomacromolecules*. Plenum Press, New York.
36 Andrade MA, Chacon PF, Merelo JJ & Moran F (1993) Evaluation of secondary structure of proteins from UV circular dichroism spectra using an unsupervised learning neural network. *Protein Eng* **6**, 383–390.
37 Bohm G, Muhr R & Jaenicke R (1992) Quantitative analysis of protein far UV circular dichroism spectra by neural networks. *Protein Eng* **5**, 191–195.
38 McGuffin LJ, Bryson K & Jones DT (2000) The PSIPRED protein structure prediction server. *Bioinformatics* **16**, 404–405.
39 Pace CN (1986) Determination and analysis of urea and guanidine hydrochloride denaturation curves. *Methods Enzymol* **131**, 266–280.
40 Del Vecchio P, Graziano G, Granata V, Barone G, Mandrich L, Ross M & Manco G (2002) Denaturing action of urea and guanidine hydrochloride towards two thermophilic esterases. *Biochem J* **367**, 857–863.
41 Mayo S & Baldwin RL (1993) Guanidinium chloride induction of partial unfolding in amide proton exchange in RNaseA. *Science* **262**, 873–876.
42 Monera OD, Kay CM & Hodges RS (1994) Protein denaturation with guanidine hydrochloride or urea provides a different estimate of stability depending on the contributions of electrostatic interactions. *Protein Sci* **3**, 1984–19891.
43 Verma A, Simard JM & Rotello VM (2004) Effect of ionic strength on the binding of α-chymotrypsin to nanoparticle receptors. *Langmuir* **20**, 4178–4181.
44 Cedervall T, Lynch I, Lindman S, Berggard T, Thulin E, Nilsson H, Dawson KA & Linse S (2007) Understanding the nanoparticle–protein corona using methods to quantify exchange rates and affinities of proteins for nanoparticles. *Proc Natl Acad Sci USA* **104**, 2050–2055.
45 Jelesarov I & Bosshard HR (1999) Isothermal titration calorimetry and differential scanning calorimetry as complementary tools to investigate the energetics of biomolecular recognition. *J Mol Recognit* **12**, 3–18.
46 Connelly PR (1994) Acquisition and use of calorimetric data for prediction of the thermodynamics of ligand-binding and folding reactions of proteins. *Curr Opin Biotechnol* **5**, 381–388.
47 De M, You CC, Srivastava S & Rotello VM (2007) Biomimetic interaction of proteins with functionalized nanoparticles: a thermodynamic study. *J Am Chem Soc* **129**, 10747–10753.

48 Gasteiger E, Hoogland C, Gattiker A, Duvaud S, Wilkins MR, Appel RD & Bairoch A (2005) Protein Identification and Analysis Tools on the ExPASy Server. *The Proteomics Protocols Handbook*. Humana Press, New York.
49 Kumar AS & Chen MS (2008) Nanostructured zinc oxide particles in chemically modified electrodes for biosensor applications. *Anal Lett* **41**, 141–158.
50 Fardad S, Massudi R, Manteghi A & Amini MM (2007) Proceedings of the 7th IEEE International Conference on Nanotechnology. August 2–5, Hong Kong.
51 Norde W & Lyklema J (1989) Protein adsorption and bacterial adhesion to solid surfaces: a colloid-chemical approach. *Colloids Surf* **38**, 1–13.
52 Zoungrana T, Findenegg GH & Norde W (1997) Structure, stability and activity of adsorbed enzymes. *J Colloid Interface Sci* **190**, 437–448.
53 Koutsopoulos S, Patzsch K, Bosker WT & Norde W (2007) Adsorption of trypsin on hydrophilic and hydrophobic surfaces. *Langmuir* **23**, 2000–2006.
54 Joshi P, Chakrabarti S, Chakrabarti P, Haranath D, Shanker V, Ansari ZA, Singh SP & Gupta V (2009) Role of surface adsorbed anoinic species in antibacterial activity of ZnO quantum dots against *Escherichia coli*. *J Nanosci Nanotechnol* **9**, 6427–6433.

Supporting information

The following supplementary material is available:
Fig. S1. Elution profile of analytical gel filtration of free and ZnO NP-conjugated ToxRp.
Fig. S2. The output from PSIPRED runs on sequence of ToxRp.
Fig. S3. (A)Tryptophan fluorescence emission of free and ZnO NP conjugated ToxRp at different pH. (B) CD spectra of free and ZnO NP conjugated ToxRp at different pH.

This supplementary material can be found in the online version of this article.

Please note: As a service to our authors and readers, this journal provides supporting information supplied by the authors. Such materials are peer-reviewed and may be re-organized for online delivery, but are not copy-edited or typeset. Technical support issues arising from supporting information (other than missing files) should be addressed to the authors.